J Fluoresc (2012) 22:323–337
DOI 10.1007/s10895-011-0963-7

ORIGINAL PAPER

Photophysics, Photochemistry and Energetics of UV Light Induced Disulphide Bridge Disruption in apo-α-Lactalbumin

Manuel Correia · Maria Teresa Neves-Petersen · Antonietta Parracino · Ane Kold di Gennaro · Steffen B. Petersen

Received: 6 June 2011 / Accepted: 30 August 2011 / Published online: 14 October 2011

Abstract Continuous 295 nm excitation of whey protein bovine apo-α-lactalbumin (apo-bLA) results in an increase of tryptophan fluorescence emission intensity, in a progressive red-shift of tryptophan fluorescence emission, and breakage of disulphide bridges (SS), yielding free thiol groups. The increase in fluorescence emission intensity upon continuous UV-excitation is correlated with the increase in concentration of free thiol groups in apo-bLA. UV-excitation and consequent SS breakage induce conformational changes on apo-bLA molecules, which after prolonged illumination display molten globule spectral features. The rate of tryptophan fluorescence emission intensity increase at 340 nm with excitation time increases with temperature in the interval 9.3–29.9 °C. The temperature-dependent 340 nm emission kinetic traces were fitted by a 1st order reaction model. Native apo-bLA molecules with intact SS bonds and low tryptophan emission intensity are gradually converted upon excitation into apo-bLA molecules with disrupted SS, molten-globule-like conformation, high tryptophan emission intensity and red-shifted tryptophan emission. Experimental Ahrrenius activation energy was 21.8±2.3 kJ.mol^{-1}. Data suggests that tryptophan photoionization from the S_1 state is the likely pathway leading to photolysis of SS in apo-bLA. Photoionization mechanism(s) of tryptophan in proteins and in solution and the activation energy of tryptophan photoionization from S_1 leading to SS disruption in proteins are discussed. The observations present in this paper raise concern regarding UV-light pasteurization of milk products. Though UV-light pasteurization is a faster and cheaper method than traditional thermal denaturation, it may also lead to loss of structure and functionality of milk proteins.

Keywords Photophysics and photochemistry of α-lactalbumin · Protein fluorescence quenching · UV-light induced disulphide bridge disruption · Activation energy of photoionization · Tryptophan photoionization in proteins

Abbreviations

A_0	Ahrrenius pre-exponential factor
apo-bLA	Ca^{2+}-depleted bovine α-lactalbumin

M. Correia · A. Parracino · A. K. di Gennaro
Department of Physics and Nanotechnology, Aalborg University, Skjernvej 4A, DK-9220 Aalborg, Denmark

M. Correia
e-mail: mc@nano.aau.dk

A. Parracino
e-mail: m.parracino@yahoo.it

A. K. di Gennaro
e-mail: ak@nano.aau.dk

M. T. Neves-Petersen (✉)
INL Int Iberian Nanotechnol Lab,
P-4715310 Braga, Portugal
e-mail: teresa.petersen@inl.int

M. T. Neves-Petersen
NanoBiotechnology Group, Department of Biotechnology, Chemistry and Environmental Sciences, Aalborg University, Sohngaardsholmsvej 57, DK-9000 Aalborg, Denmark
e-mail: tnp@bio.aau.dk

S. B. Petersen
NanoBiotechnology Group, Department of Health Science and Technology, Aalborg University,
Fredrik Bajers vej 7, DK-9220 Aalborg, Denmark
e-mail: sp@hst.aau.dk

S. B. Petersen
The Institute for Lasers, Photonics and Biophotonics, University at Buffalo, The State University of New York Buffalo, Buffalo, NY 14260-3000, USA

apo-LA	Ca^{2+}-depleted α-lactalbumin
bLA	bovine α-lactalbumin
CD	circular dichroism
Cys	C, cysteine
DTNB	5,5′-dithiobis-2-nitrobenzoic acid
E_a	Ahrrenius activation energy
e^-_{aq}	solvated electron
k	rate fluorescence emission intensity increase at 340 nm
Gly	Glycine
LA	α-lactalbumin
LAMI	light assisted molecular immobilization
Phe	phenylalanine
S_1	relaxed first electronic singlet state
S*	non-relaxed pre-fluorescent first electronic singlet state
SS	disulphide bridge(s)
TNB^{2-}	2-nitro-5-thiobenzoate ion
Trp	W, tryptophan
^{T}Trp	tryptophan triplet state
Tyr	tyrosine
UV	ultraviolet
Δλ	difference in wavelength
λ_{max}	wavelength at maximum fluorescence emission
MG	molten globule

Introduction

Several reviews have been published on the photochemistry and photophysics of tryptophan (Trp) [1, 2] tyrosine (Tyr) [3, 4] phenylalanine (Phe) [5] and cystine [6]. Excitation to higher energy states is followed by relaxation to ground state (e.g. fluorescence, phosphorescence) or to excited state photochemical or photophysical processes, such as photoionization [2]. Since in this work the protein has been excited at 295 nm, we will focus on Trp photochemistry. Trp side-chain has the highest absorption at 280 and 287 nm [7]. Upon Trp excitation the following intermediates are formed [1, 8, 9]: excited singlet state S_1 and/or higher S^* excited states (schemes 1, 2); solvated electrons e^-_{aq}, formed upon electron ejection to the solvent (scheme 3–6); tryptophan radical cation $Trp^{\bullet+}$ which rapidly deprotonates yielding the neutral radical $Trp^{\bullet}$ (scheme 7) which can react with molecular oxygen, Tyr or cystine leading to peptide chain cleavage; ^{T}Trp, formed upon intersystem crossing from S_1 into triplet-state (scheme 8); protonated triplet state formed after intramolecular proton transfer from protonated NH_3^+ group to the indole ring (scheme 9).

$$^{S_0}Trp + h\nu \rightarrow {}^{S_1}Trp \quad (1)$$

$$^{S_0}Trp + h\nu \rightarrow {}^{S^*}Trp \quad (2)$$

$$^{S^*}Trp \rightarrow Trp^{\bullet+} + e^-_{aq} \quad (3)$$

$$^{S^*}Trp \rightarrow {}^{S_1}Trp \quad (4)$$

$$^{S_1}Trp \rightarrow Trp^{\bullet+} + e^-_{aq} \quad (5)$$

$$^{S_1}Trp + h\nu \rightarrow {}^{S_1}Trp^{\bullet+} + e^-_{aq} \quad (6)$$

$$Trp^{\bullet+} \rightarrow Trp^{\bullet} + H^+ \quad (7)$$

$$^{S_1}Trp \rightarrow {}^{T}Trp \quad (8)$$

$$^{S_1}Trp + H^+ \rightarrow {}^{T}TrpH^+ \quad (9)$$

Trp photoionization, a major photo-oxidation pathway of many proteins [10, 11], can take place from the pre-

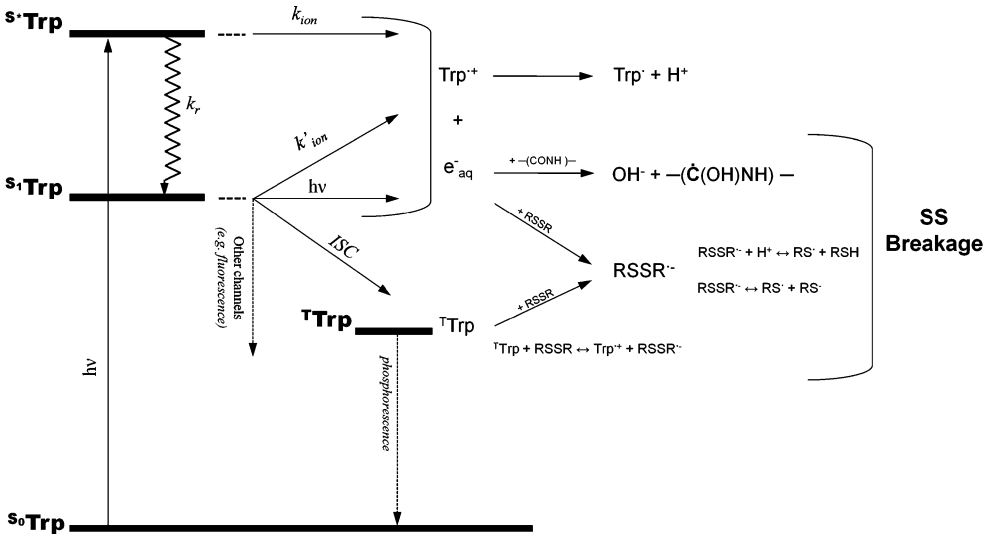

Fig. 1 Photophysical and photochemical pathways of Trp in proteins upon UV excitation. Pathways were assembled from articles from Bent and Hayon [1], Neves-Petersen et al. [10], Sherin et al. [14, 15] and Kerwin and Remmele [16]

fluorescent state S^* and/or from S_1 (Fig. 1). Ionization from S^* (rate constant k_{ion}) will compete with relaxation to S_1. Ionization from S^* has been proved by flash photolysis studies of Trp in solution, being solvated electrons observed within 200 fs after excitation [12, 13]. Photoionization from S_1 (rate constant k'_{ion}) has been reported to have an Arrhenius activation energy E_a~50 kJ.mol^{-1} [14]. Ionization quantum yield from S^* has been observed to decrease with temperature increase, in sharp contrast with the yield of ionization from S_1 state, which increases with temperature increase [15].

An important photochemical mechanism in proteins involves reduction of disulphide bridges (SS) upon UV excitation of Trp and Tyr side chains [10, 16, 17]. UV-excitation of these residues leads to photoionization and generation of solvated electrons [1–4, 10, 16]. These can subsequently undergo fast geminate recombination with their parent molecule or can be captured by electrophilic specii like cystines, molecular oxygen or H_3O^+. Capture of the solvated electrons by cystines leads to the formation of $RSSR^{\bullet-}$ (disulphide electron adduct) and likely SS breakage (schemes 10, 11) [18]. Solvated electrons can also interact with the peptide chain creating hydroxide ions and ketyl radicals (scheme 12), which can propagate along the peptide chain [1]. If a ketyl radical gets trapped by a disulfide bridge, this again results in a disulphide anion and likely SS breakage. ^{T}Trp can react with molecular oxygen to yield $Trp^{\bullet+}$ and $O_2^{\bullet-}$ [16] or it can transfer an electron to a nearby SS to give $Trp^{\bullet+}$ and $RSSR^{\bullet-}$ (scheme 13) [1]. Protonation of disulphide anion can also lead to SS disruption (scheme 14) [18].

$$e^-_{aq} + RSSR \rightarrow RSSR^{\bullet-} \tag{10}$$

$$RSSR^{\bullet-} \Leftrightarrow RS^{\bullet} + RS^- \tag{11}$$

$$e^-_{aq} + -CONH- \rightarrow OH^- + -\dot{C}(OH)NH- \tag{12}$$

$$^T Trp + RSSR \rightarrow Trp^{\bullet+} + RSSR^{\bullet-} \tag{13}$$

$$RSSR^{\bullet-} + H^+ \Leftrightarrow RS^{\bullet} + RSH \tag{14}$$

Reduction of SS upon UV excitation of aromatic residues has been shown for proteins such as cutinase and lysozyme [10, 17, 19], bovine serum albumin [20, 21] prostate specific antigen [22], and antibody Fab fragments [23]. This phenomenon has lead to a new technology for protein immobilization (LAMI, light assisted molecular immobilization) since the created thiol groups can bind thiol reactive surfaces leading to oriented covalent protein immobilization [19–31].

α-lactalbumin (LA) is a small (~14.2 kDa), acidic (isoelectric point ~4–5) protein present in the milk whey of mammalians. Most mammalian LAs share a highly conserved 3D structure [32, 33]. Expressed exclusively during lactation, LA plays an important role in lactose biosynthesis [32–34]. LA unfolding has been extensively studied since the protein adopts molten globule (MG) conformations under mild denaturating conditions [35, 36]. In the MG state the protein is still compact, with native-like secondary structure, but lacks well defined tertiary interactions, and the hydrophobic regions are more solvent accessible [36]. Calcium-bound LA is the major form under physiological conditions [33]. The Ca^{2+} depleted form of LA (apo-LA) herein studied is involved in other functions besides lactose synthase regulation, such as interaction with lipid membranes [37] and oleic acid [36]. The latter can give rise to a multimeric form that can induce apoptosis in tumor cells [38–40]. Apo-LA conformation is extremely sensitive to experimental conditions, particularly pH and ionic strength. It is known to adopt different conformations in solution such as molten globule forms void of cooperative thermal transition or partly native folded states showing cooperativity upon thermal denaturation [32, 36, 41–45]. At high ionic strength bovine apo-LA (apo-bLA) shows minor structural differences compared to native calcium-bound LA [32, 45]. Upon Ca^{2+} removal, the electrostatic interactions at the Ca^{2+} binding site are disrupted, leading to local structural destabilization of the protein structure [32]. Positively charged ions (e.g. Na^+, K^+) will interact with the negatively charged residues of the Ca^{2+} binding site and stabilize the protein structure [32, 45, 46]. Bovine LA (bLA) displays a marginal thermodynamic folding barrier, which is apparently modulated by protein electrostatics in its apo-form [47]. This low folding barrier explains the conformational flexibility of apo-LA in solution [47]. Apo-LA can be perceived as a continuum of conformational states, an ensemble of conformations whose population distribution depends strongly on electrostatic interactions.

Apo-bLA has 4 Trp residues in close spatial proximity of disulphide bridges, making it a good candidate for studying light induced SS disruption mediated by Trp excitation. UV light induced SS disruption in LA upon Trp excitation has been verified for Ca^{2+} bound and apo-versions of bovine and human LA [48], and goat LA [49, 50]. Mass-spectroscopy confirmed light induced SS disruption in human and goat LA [48–50]. SS disruption was correlated with a red-shift in fluorescence emission as well as with an increase in fluorescence yield [48, 49]. We here show for the first time the correlation between fluorescence emission increase and UV-light induced breakage of SS in apo-bLA. We report the photophysics, photochemistry, structural and fluorescence spectral changes induced by 295 nm excitation

of Trp residues in apo-bLA. The studies have been carried out at different temperatures in order to obtain the Arrhenius activation energy of such process. For the first time to our knowledge we here report the activation energy of photochemical process(es) leading to SS disruption upon excitation of aromatic residues in proteins. Trp photoionization mechanism(s) and consequent induced disruption of disulphide bridges in apo-bLA are discussed.

Materials and Methods

Protein and Buffer Solutions

Apo-bLA from bovine milk type III was purchased from Sigma-Aldrich (product L6010). Apo-bLA concentrations were determined by Abs_{280nm} using an extinction molar coefficient of 28500 $M^{-1}.cm^{-1}$ [48, 51]. Trizma base (Sigma) was used for preparation of Tris HCl buffers. pH adjustments were carried out by addition of 2.5 M HCl. Tris HCl buffer displays a minimal pH drift with temperature changes. Milli-Q water with conductivity below 0.2 $\mu S.cm^{-1}$ was used.

Fluorescence Emission of apo-bLA as a Function of 295 nm Excitation Time

UV-light triggered reaction mechanisms in apo-bLA were probed by monitoring the time-dependent fluorescence emission intensity at 340 nm of LA upon 295 nm excitation. 1.86 μM apo-bLA was prepared in 25 mM Tris HCl pH 8.55. 3 ml were placed in a quartz macro cuvette (1 cm path length) and excited at 295 nm during 1 h, 2 h, 3 h, 4 h, and 5 h. A fresh sample was used for each time based study. Excitation was carried out in a RTC 2000 PTI spectrometer (Photon Technology International, Canada, Inc.347 Consortium Court London, Ontario N6E 2S8) with a T-configuration, using a 75-W Xenon arc lamp coupled to a monochromator. Cuvette temperature was kept at 25 °C using a peltier element. Samples were magnetically stirred at 900 rpm in order to secure homogeneous excitation. All slits were set to 5 nm. Lamp power at 295 nm was 252 μW at the focal point in the sample holder location. After each illumination, emission and excitation spectra were recorded. Emission spectra were acquired with 295 nm and 280 nm excitation. Emission was fixed at 340 nm in detector-1 and at 320 nm in detector-2 while acquiring the excitation spectra. The same emission and excitation spectra were acquired for a non-illuminated solution and for the buffer. Raman signal was subtracted from each emission spectrum.

Detection of Free Thiol Groups Formed Upon UV Illumination of apo-bLA

Detection of free thiol groups was carried out using the Ellmann assay [17, 52]. Ellmann's reagent, 5,5′-dithiobis-2-nitrobenzoic acid (DTNB) was purchased from Invitrogen. 1 mM solution was prepared in Tris HCl, 100 mM at pH 6.6 in order to favor dissolution. The supernatant phase was used as stock solution and stored at 4 °C. The stock concentration (0.7 mM) was determined by absorbance at 324 nm using an extinction molar coefficient for DTNB in Tris HCl of 16600 $M^{-1}.cm^{-1}$ [53].

An excess of DTNB (100 μL of 0.7 mM stock solution) was added to 900 μL of illuminated solution immediately after each time-dependent 295 nm excitation, and to 900 μL of non-illuminated apo-bLA. Absorbance at 412 nm by the released 2-nitro-5-thiobenzoate ion (TNB^{2-})was monitored with a UV/Visible spectrophotometer (UV1 VWR International—Thermo Electron Corporation, Thermo Fisher Scientific Inc. 81 Wyman Street Waltham, MA 02454), using 1 cm path quartz cuvette. Absorbance at 412 nm, proportional to the amount of thiol groups present in solution, was monitored immediately after mixing the two components and a reading was obtained upon signal stabilization. The sample was kept in the dark between measurements and manually stirred before each reading. Abs_{412nm} stabilized after ~20 min of reaction. Abs_{412nm} at 22 min of reaction was used. The values were corrected for the contributions of apo-bLA and DTNB for Abs_{412nm}. Abs_{412nm} was monitored for a protein blank (900 μL of fresh 1.86 μM apo-bLA solution and 100 μL of 100 mM Tris HCl, pH 6.7) and a reagent blank (900 μL of 25 mM Tris HCl pH 8.5 and 100 μL of 0.7 mM stock solution of DTNB in Tris HCl). Concentration of thiol groups was determined using an extinction molar coefficient for TNB^{2-} of 14150 $M^{-1}.cm^{-1}$ at 412 nm [52]. The average number of free thiol groups detected per protein molecule was then estimated for each illuminated and non-illuminated samples, by dividing the concentration of detected thiol groups with the apo-bLA concentration used.

Time-Dependent Fluorescence Emission of apo-bLA at Different Temperatures

Time-based fluorescent emission kinetic traces (340 nm) obtained upon continuous 295 nm excitation of the protein solution were carried out at different temperatures (9.3, 12.9, 15.6, 20.4, 24.9 or 25.2, 29.9 or 34.6 °C) in the same RTC 2000 PTI spectrometer setup. 3 ml of 1.85 μM (runs at 9.3, 12.9, 15.6, 20.4, 24.9, 29.9 or 34.6 °C) and 3 ml of 1.66 μM (run at 25.2 °C) apo-bLA solutions (in 25 mM Tris-HCl pH 8.5) were continuously illuminated during 3.5 h in a 1 cm path quartz cuvette with constant magnetic stirring at 900 rpm.

Real-time correction was enabled in order to correct for oscillations in lamp intensity (gain set at 1.81 V). Emission spectra were acquired after each run (exc. 295 nm) at the run's temperature. Correspondent emission spectra were carried out for non-illuminated apo-bLA solutions at the same temperatures, and for the buffer, in order to Raman correct each emission spectrum. Solution temperature was previously set using a peltier element. Slits were set at 5 nm.

Circular Dichroism Measurements

Circular Dichroism (CD) spectroscopy was used to monitor the relative changes in ellipticity after 295 nm excitation of apo-bLA up to 2.8 h illumination. A solution of apo-bLA (11.5 μM in 10mM Tris HCl pH 8.55, 3.5 mL initial volume) was excited in the previously described RTC 2000 PTI spectrometer setup, using the same excitation slit width, and magnetic stirring speed. At discrete times in the excitation session, 300 μl of illuminated apo-bLA were removed and placed in a quartz microcuvette with a path length of 0.1 cm. Far-UV CD spectra (200–240 nm) of fresh and illuminated protein were acquired using the following parameters: 0.5 nm band width, resolution 1.0, 3 accumulations, scan speed 5 nm/min, 100 mdeg sensitivity, 1 s response time. Each measurement was controlled by the JASCO J-700 hardware manager (JASCO Corporation, 2967–5 Ishikawa-cho Hachioji-shi, Tokyo, Japan). The buffer signal was subtracted from all spectra.

Protein Three-Dimensional Structure Representation, Accessible Surface Area of Trp Residues and Trp-SS Distances

The crystallography data used for 3D protein representation, accessible surface area (ASA) and distance calculations was extracted from the PDB files 1F6S (apo-bLA crystallized at high ionic strength) and 1F6S.pdb (native bLA) [32]. Apo-bLA 3D structure was displayed using Accelrys Discovery Studio Visualizer 2.5. The ASA values for each Trp residue were calculated using the program *Surface Racer*© considering the probe radius of 1.4 Å (approximate value for a water molecule radius), and the van der Vaals radii sets of Richards—1977 [54, 55]. The ASA of Trp in the tripeptide Gly-Trp-Gly estimates the total ASA of this residue with the main chain in an extended conformation. The value used as Trp ASA in Gly-Trp-Gly was 217 $Å^2$, according to Miller et al. [56]. Distances between Trp residues and potential quenching groups were calculated in Rasmol 2.6 using the "monitor" tool.

Data Analysis

All smoothing procedures were carried out by adjacent averaging in Origin 8.0. Fluorescence emission and far-UV CD spectra were smoothed using a 5 points adjacent average, while excitation spectra were smoothed using 2 points adjacent average prior to normalization. Normalized emission and excitation spectra were obtained by dividing each data point by the maximum intensity value in each spectrum. Normalized time-based fluorescence measurements were obtained by dividing each data point (emission intensity) by the time zero emission. Normalized fluorescence kinetic traces obtained upon 295 nm excitation for 3.5 h at different temperatures were fitted with an exponential function $F(t) = C_1 - C_2 e^{-kt}$, where *F(t)* is the fluorescence emission intensity at 340 nm at the 295 nm excitation time t, C_1 and C_2 are constants and k is the rate constant fluorescence emission intensity increase. The first 800 s were excluded while fitting all kinetic traces since an initial decrease in fluorescence emission intensity is observed. Fittings were carried out from 800 s till the time corresponding to 95% of maximum fluorescence emission in order to avoid the region where fluorescence emission intensity peaks. The temperature dependence of the rate constant for fluorescence emission increase at 340 nm (k) was studied by fitting the data values with the logarithmic form of the Arrhenius equation $\ln k = \ln A_0 + \frac{E_a}{RT}$, where A_0 is the pre-exponential factor, E_a the activation energy, R the universal constant for perfect gases and T the temperature . The fitting took into account the standard errors determined for each previously calculated k value. Each data point was associated with a weight, $w_i = 1/\sigma_i^2$, where σ_i is the error bar size for each data point. Data fitting and plotting were done in Origin 8.0.

Results

Three-Dimensional Structure of bLA

Apo-bLA 3D structure obtained upon crystallization at high ionic strength [32] is displayed in Fig. 2. Apo-bLA 3D structure has high structural homology with the crystallized structure of native Ca^{2+}-bound bLA. The root mean square deviation obtained after superimposition of the two structures is of only 0.68 Å [32]. LA fold displays two sub-domains separated by a cleft: a large α-helical sub-domain (Fig. 2, in red on the online color version, and in light grey on the black and white version) formed by three main α-helices and two short 3_{10} helices, and a small β-sheet sub-domain (Fig. 2, in blue on the online color version, and in dark grey on the black and white version) constituted by non-structured loops, a small three-stranded anti-parallel β-pleated sheet and a short 3_{10} helix [32] (Fig. 2). The tertiary structure of LA is further stabilized by four SS (Fig. 2, stick configuration, in green on the online color version, and in white on the black and white version). Cys73-Cys91 holds together the two sub-domains. Cys61-Cys77 links nonstructured loops, connect-

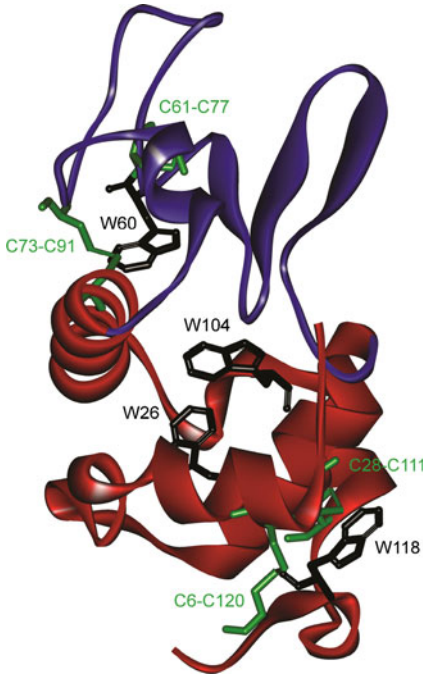

Fig. 2 3D structure of bovine apo-α-lactalbumin crystallized at high ionic strength (1F6S.pdb) [32]. 4 Trp (W) and 8 Cys (C) involved in 4 disulphide bridges (SS) are displayed (color online)

ing both sub-domains as well and is located in the β-sheet subdomain. Cys6-Cys120 and Cys28-Cys111 are situated in the α-helical sub-domain [33].

bLA contains four Trp residues (Fig. 2, stick configuration, in black) that are located within the two hydrophobic clusters of the protein, being part of two separate aromatic clusters [57]. Trp26, Trp60, and Trp104 belong to the aromatic cluster II. In the 3D structure of native bLA, the accessible solvent areas (ASA) of these Trp residues account for respectively 0.95, 2.70 and 13.96% of the total ASA of Trp in the tripeptide Gly-Trp-Gly. The correspondent values in crystallized apo-bLA are 0, 0.06 and 4.35%. The low relative values of ASA indicate that in the crystallized lattice of bLA these Trp residues are buried, even when the protein is Ca^{2+}depleted. Trp118 is situated in aromatic cluster I and is more solvent exposed, displaying 13.96 and 12.32% of the ASA of Trp in Gly-Trp-Gly for native and apo-bLA respectively.

In the apo-bLA 3D crystal structure Trp residues are surrounded by potential fluorescence quenching groups (Table 1). Trp60 is in van der Waals contact (≤ 5.2 Å as defined by Li and Nussinov [58]) with Cys73-Cys91 (4.20 Å) and 6.24 Å away from Cys61-Cys77. Trp118 is in van der Waals contact with Cys28-Cys111 (4.74 Å). The closest distance between Trp104 and a SS bond is 7.93 Å. Trp 60 and Trp104 are also in van der Waals contact to other potential quenching groups, the peptide bonds of Lys94-Ile95 (4.09 Å) and Val92-Lys93 (5.08 Å) respectively. Similarly, Trp118 is direct contact with imizidole ring of His32

Table 1 Distances between Trp residues and its potential quenchers in the 3D crystallized structures of native and apo-bLA (at high ionic strength).The values correspond to the shortest distances between the atoms involved in the quenching of Trp residues and the indole side-chain atoms of Trp residues. In bold are highlighted the Trp-quencher pairs for which there is direct van der Vaals contact (≤ 5.2 Å as defined by Li and Nussinov [58])

Pair		Distance (Å)	
Tryptophan	Potential Quencher	Apo-bLA	Native bLA
Trp26	**Trp104**	**3.61**	**3.78**
Trp26	Cys28-Cys111	8.38	8.37
Trp26	Cys6-Cys120	13.36	14.81
Trp60	Cys61-Cys77	6.24	6.43
Trp60	**Cys73-Cys91**	**4.20**	**4.67**
Trp60	**Peptide bond of Lys94-Ile95**	**4.09**	**3.76**
Trp104	**Peptide bond of Val92-Lys93**	**5.08**	**5.06**
Trp104	Cys28-Cys111	8.95	9.06
Trp104	Cys73-Cys91	7.93	7.80
Trp118	Cys6-Cys120	8.07	9.60
Trp118	**Cys28-Cys111**	**4.74**	**5.15**
Trp118	**His32**	**4.12**	**3.86**
Trp118	Peptide bond of Val27-Cys28	5.70	5.70

(4.12 Å) and close to the peptide bond Val27-Cys26 (5.70 Å). In its protonated form, the imidazole ring of histidine is known to quench substantially Trp fluorescence in proteins [59, 60]. The indole side-chains of Trp26 and Trp104 are also in van der Waals contact (3.61 Å), allowing for resonance energy transfer. Similar distances are observed for the structure of native bLA. The same structural features have been pointed out by Vanhooren et al. for native goat LA [61].

Steady State Fluorescence Emission

Fluorescence emission intensity of apo-bLA (340 nm) upon continuous 295 nm excitation is displayed in Fig. 3. A rapid increase in fluorescence emission intensity (~17%) is observed after 1.7 h of illumination, peaking at ~2.7 h.

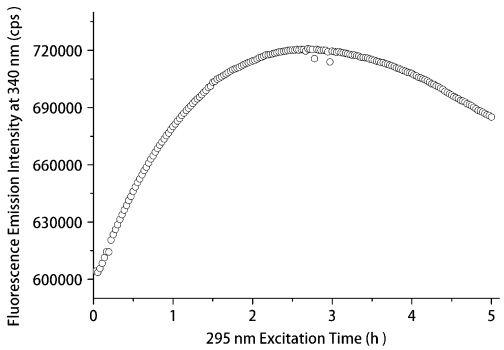

Fig. 3 Fluorescence emission intensity of apo-bLA versus 295 nm illumination time. Emission was monitored at 340 nm

Afterwards, fluorescence emission intensity decreases with further illumination.

Excitation spectra (em. 340 nm) and emission spectra (exc. 295 nm) were acquired prior and after 1–5 h excitation at 295 nm. The observed increase in fluorescence excitation intensity is correlated with an increase in fluorescence emission intensity for the first 2 h of 295 nm excitation (Fig. 4a). Furthermore, the longer the illumination time the larger the fluorescence emission red-shift (Fig. 4a and d).

Normalized excitation spectra with emission set at 340 nm and 320 nm acquired after apo-bLA 295 nm excitation for different illumination times are displayed in Fig. 4b and c, respectively. A progressive decrease in

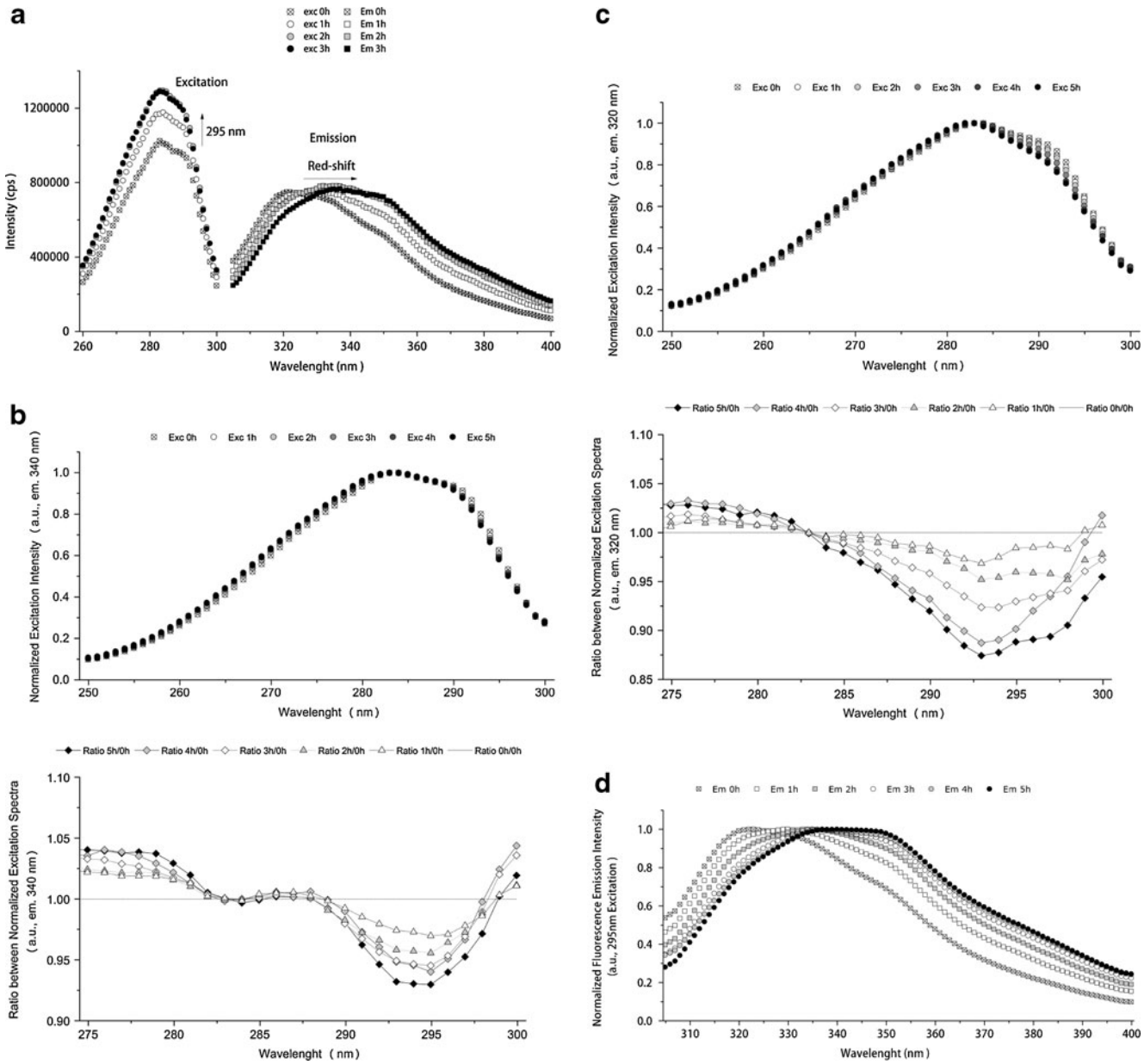

Fig. 4 **a**. Effect of 295 nm excitation time on excitation and emission intensity spectra. Excitation spectra were acquired fixing emission at 340 nm and emission spectra were acquired upon excitation at 295 nm. **b**. Top panel: Normalized excitation spectra of apo-bLA acquired after 0–5 h 295 nm illumination with emission at 340 nm; bottom panel: ratio between normalized excitation spectra displayed in the top panel (ratio between each excitation spectrum acquired after a specific illumination time and the excitation spectrum of non-illuminated apo-bLA sample). **c** Top panel: Normalized excitation spectra of apo-bLA acquired after 0–5 h 295 nm illumination with emission at 320 nm, respectively; bottom panel: ratio between normalized excitation spectra displayed in the top panel (ratio between each excitation spectrum acquired after a specific illumination time and the excitation spectrum of non-illuminated apo-bLA sample). **d** Normalized emission spectra of apo-bLA illuminated for different time periods and non-illuminated apo-bLA. Excitation was carried out at 295 nm

normalized excitation intensity with increasing illumination time is observed at 290–297 nm, wavelengths that only excite Trp (Fig. 4b, bottom panel). Figure 4c (top panel) shows a progressive decrease in normalized excitation intensity with increasing illumination time for wavelengths higher than 283 nm. The ratio between normalized excitation spectra (Fig. 4c, bottom panel) shows a progressive loss of intensity between 285 nm and 300 nm, wavelengths where Trp and Tyr are excited. After 5 h illumination, the ratio between normalized excitation spectra shows a 7.0% decrease in normalized excitation intensity at 295 nm when emission has been set at 340 nm (Fig. 4b) compared to 11.2% decrease when emission has been set at 320 nm (Fig. 4c).

A progressive red-shift in fluorescence emission is observed upon illumination (Fig. 4d). Non-illuminated apo-bLA displays maximum fluorescence emission at ~322.9 nm. After 5 h of excitation, this maximum is red-shifted to ~339.9 nm (Table 3 and Fig. 4d).

Thiol group's Quantification

The concentration of solvent accessible thiol groups in apo-bLA has been determined with Ellmann's reaction for a non-illuminated sample and for samples previously illuminated at 295 nm during 1–5 h at 25 °C. An increase in the average number of detected thiol groups per protein molecule is correlated with the increase in fluorescence emission intensity as a function of 295 nm illumination time (Fig. 5). The average number of detected thiol groups rapidly increases in the first 3 h of illumination, which is correlated with an exponential increase in fluorescence emission intensity (Fig. 5). After fluorescence maximum intensity is reached, a further increase in the average number of thiol detected thiol groups is observed (between 3 and 4 h of illumination). Data confirms that excitation of Trp residues in apo-bLA induces SS disruption. Ellmann's reaction also confirmed the presence of thiol formation in apo-bLA illuminated for 3.5 h with 295 nm light at different temperatures (9.3, 12.9, 15.6, 20.4, 24.9, 29.9 and 34.6 °C).

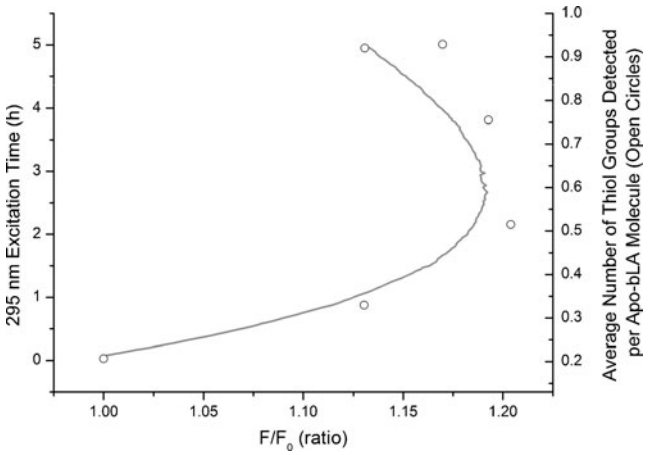

Fig. 5 Average number of free thiol groups detected per apo-bLA molecule (open circles) *versus* relative increase in fluorescence emission intensity (F/F_0) of apo-bLA with 295 nm excitation time. In gray is displayed fluorescence emission increase at 340 nm (F/F_0) versus 295 nm excitation time. Detection of free thiol groups was carried out using the Elmann's assay. The average number of free thiol groups formed upon UV-excitation the protein was estimated from the absorbance of the product of the Elmann's Assay reaction, TNB^{2-}, at 412 nm

CD Measurements

Far-UV CD spectra of fresh and 295 nm illuminated apo-bLA show that progressive Trp excitation (2.8 h) results only in minor changes in the secondary structure of the protein (12.33% signal loss at 222 nm, data not shown).

Temperature Dependent Studies

In order to study the temperature dependence of photoinduced reaction mechanisms in apo-bLA, fluorescence emission kinetic traces have been acquired at different temperatures. Kinetic traces recorded at 9.3, 12.9, 15.6, 20.4, 25.2 and 29.9 °C are displayed in Fig. 6a (gray and black lines). All traces display a strong initial increase in fluorescence emission intensity, peaking after a few hours. Afterwards, the fluorescence emission intensity is observed to decay upon further 295 nm illumination. At 34.6 °C, apo-bLA fluorescence emission intensity decreases upon excitation (data not shown). In Fig. 6a it can be observed that the largest total fluorescence emission increase is observed after illumination at the lowest temperature (9.3 °C). For the three lowest temperatures fluorescence emission increases more than 25%. Additionally, the higher the temperature the lower the maximum fluorescence emission intensity is. On the other hand, the higher the temperature, the steeper the initial slope of fluorescence emission increase is, indicating an increase in the rate of fluorescence emission increase k (see paragraph below and Table 2).

Fitted kinetic traces are displayed in Fig. 6a (color traces on the online version, and black lines on the black and white version). Fitted parameters and root mean square deviation (R^2) are displayed in Table 2. Both constants C_1 and C_2 decrease with temperature increase, whereas the rate constant k increases with temperature. In the exponential model used the constant C_1 defines the maximum fluorescence intensity emission. The fluorescence emission intensity is directly proportional to the value of C_1 in the whole time-trace. C_2 affects both the initial value of fluorescence emission intensity (value at time zero) and the steepness of the slope of fluorescence emission intensity increase. The

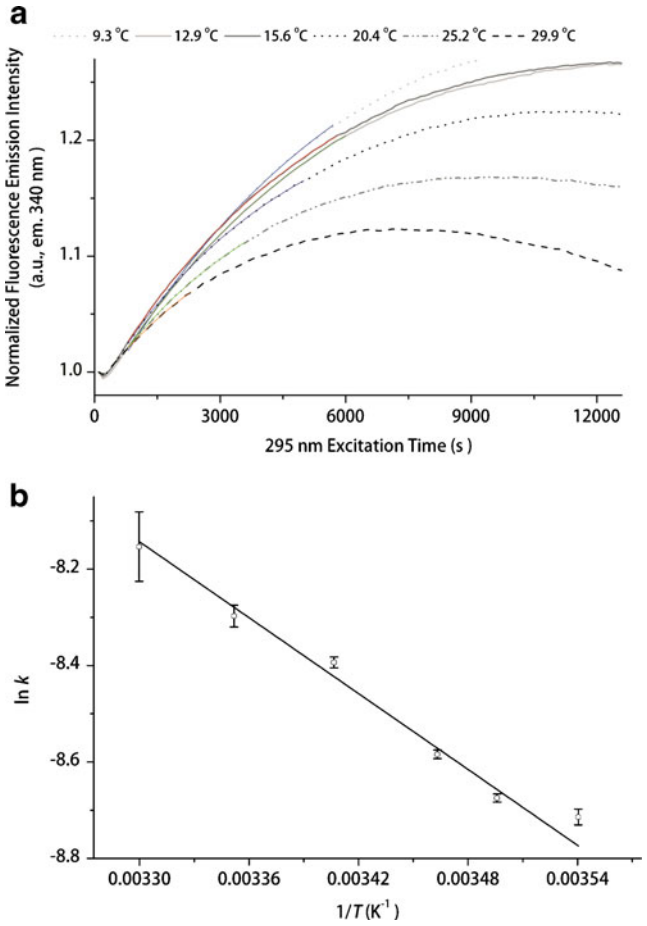

Fig. 6 **a** Black and white kinetic traces: apo-bLA experimental fluorescence emission intensity (em 340 nm) as a function of 295 nm illumination time at different temperatures (9.3, 12.9, 15.6, 20.4, 25.2, and 29.9 °C). Highlighted traces: fitting of experimental data from 800 s till the time corresponding to 95% of maximum fluorescence emission intensity. Fitting was carried out using an exponential function $F(t)=C_1\text{-}C_2.e^{-kt}$. Fitted parameter values and correspondent errors, and root mean square error value were obtained after fitting each kinetic trace. **b** Arrhennius plot showing the linear correlation between the logarithm of the rate constant ln k and the inverse of temperature $1/T$ (R^2=0.98429). Calculated parameters: E_a=21.8± 2.3 kJ.mol^{-1} and A_0=1.67±1.57 s^{-1}. Uncertainty errors for ln k values are displayed with error bars

higher the value of C_2 the fastest the fluorescence emission intensity increase is. The rate constant k does not influence the magnitude of the fluorescence emission intensity increase. The highest the rate constant k, the fastest the fluorescence emission intensity increase is. In Fig. 6b is displayed the Arrhenius plot of the experimental k values. The observed linear regression shows that k is temperature dependent following Arrhenius law. Activation energy (Ea) and pre-exponential factor (A_0) calculated from the slope ($-Ea/R$) and the $ln\ A_0$ were respectively 21.8±2.3 kJ. mol^{-1} and 1.67±1.57 s^{-1}.

In Fig. 7 are displayed the fluorescence emission spectra (exc 295 nm) for non-illuminated apo-bLA (A) and after 3.5 h of 295 nm illumination (B) at each temperature. Maximum fluorescence intensity of non-illuminated apo-bLA is observed at 322.9 nm at temperatures between 9.3 and 29.9 °C (A, Table 3). Fluorescence emission at 34.6 °C becomes 11 nm red-shifted (A, Table 3). Fluorescence emission intensity at 340 nm increases linearly with decreasing temperature between 9.3 and 29.9 °C: F_{340nm}=−6742 T+ 765787, R^2=0.95. After 3.5 h of 295 nm illumination, fluorescence emission becomes red-shifted at all temperatures (B). The largest shifts are observed between 12.9 and 29.9 °C, ranging between 13 and 17 nm (Table 3). A 5 nm red shift is observed at 34.6 °C.

Discussion

Non-illuminated apo-bLA at pH 8.55 and 25 °C shows maximum Trp fluorescence emission at 322.9 nm (295 nm excitation, Fig. 4a and Table 3), a value close to the maximum of emission of Ca^{2+}-bound bLA at 325 nm (300 nm excitation and neutral pH) [62]. The aromatic clusters I and II contain approximately half of the residues involved in the packing of the two hydrophobic clusters of bLA, which makes Trp suited to serve as solvent accessibility reporter group to study structural changes in hydrophobic regions of the protein [57]. In native goat LA Trp26 is the strongest contributor for Trp fluorescence, due to the lack of direct quenching compared to the other Trp residues [61]. Trp26 belongs to the aromatic cluster II, which includes also Trp60 and Trp104. These Trp residues are quite protected from the solvent in native bLA as shown by the calculated ASA values (see Results section) and previous crystallography, NMR and hydrogen exchange

Table 2 Fitted parameter values and correspondent errors, and root mean square value obtained after fitting each temperature dependent 340 nm fluorescence emission kinetic trace displayed in Fig. 6a to the equation $F(t) = C_1 - C_2e^{-kt}$

T (°C)	C_1	C_2	k (s^{-1})	R^2
9.3	1.37±0.004	0.402±0.003	1.64E-04±2.73E-06	0.99986
12.9	1.33±0.002	0.356±0.001	1.71E-04±1.44E-06	0.99995
15.6	1.32±0.002	0.340±0.001	1.87E-04±1.67E-06	0.99994
20.4	1.25±0.002	0.274±0.001	2.26E-04±2.57E-06	0.99992
25.2	1.20±0.003	0.221±0.002	2.49E-04±5.64E-06	0.99989
29.9	1.16±0.008	0.174±0.007	2.88E-04±2.07E-05	0.99977

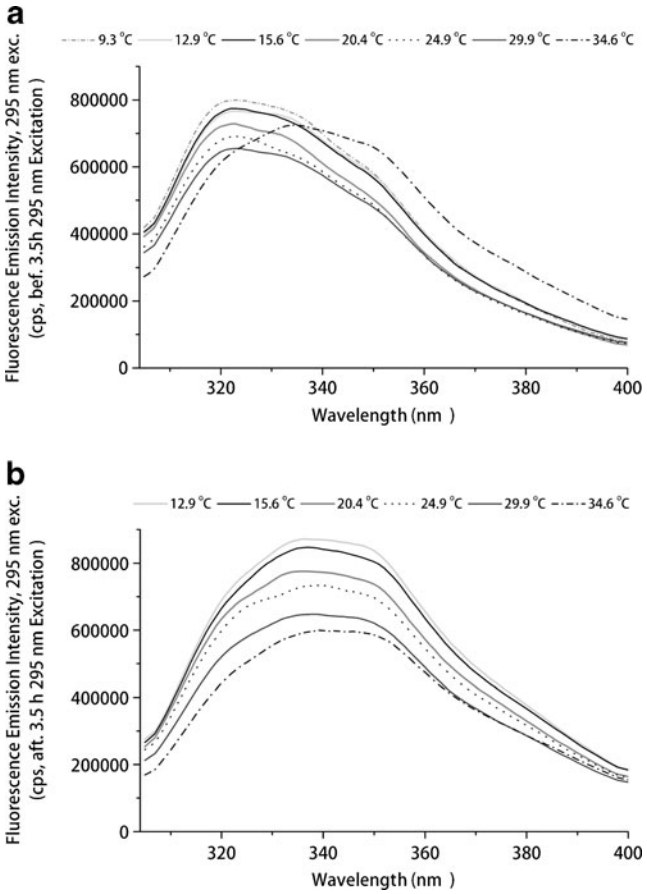

Fig. 7 **a** Emission spectra (exc 295 nm) of apo-bLA acquired before 295 nm illumination (fresh solutions) at different temperatures (9.3, 12.9, 15.6, 20.4, 24.9, 29.9 and 34.6 °C). **b** Fluorescence emission intensity spectra (exc 295 nm) of apo-bLA acquired after 3.5 h of 295 nm illumination at different temperatures (9.3, 12.9, 15.6, 20.4, 24.9, 29.9 and 34.6 °C)

Table 3 Effect of 295 nm excitation time and temperature on the wavelength at maximum fluorescence emission ($\lambda_{max\ emission}$) of apo-bLA (data displayed in Fig. 4d, 9A and 9B). Data was acquired at pH 8.55

Fig. 4d	Illum. time (h)	$\lambda_{max\ emission}$ (nm)	$\Delta\lambda$ ($\lambda_{after\ illumination} - \lambda_{0h\ illumination}$) (nm)
	0	322.9	-
	1	329.9	7
	2	333.9	11
	3	334.9	12
	4	336.9	14
	5	339.9	17
Fig. 7a	T (ºC)	$\lambda_{max\ emission}$ (nm)	$\Delta\lambda$ ($\lambda_{Ti} - \lambda_{T=9.3\,°C}$) (nm)
	9.3	322.9	0
	12.9	322.9	0
	15.6	322.9	0
	20.4	322.9	0
	24.9	322.9	0
	29.9	322.9	0
	34.6	333.9	11
Fig. 7b	T (ºC)	$\lambda_{max\ emission}$ (nm)	$\Delta\lambda$ ($\lambda_{after\ 3.5h\ exc.} - \lambda_{0h\ exc}$) (nm)
	9.3	-	-
	12.9	335.9	13
	15.6	336.9	14
	20.4	335.9	13
	24.9	339.9	17
	29.9	337.9	15
	34.6	338.9	5

experiments studies [32, 45]. There is no major shift in wavelength of maximum Trp fluorescence emission or considerable changes in the spectrum shape for apo-bLA reported here compared to the native Ca^{2+} bound protein [62]. This indicates that the Trp residues remain buried.

At high ionic strength there are no significant differences in Trp solvent exposure between native and apo-bLA, as suggested by the calculated ASA values and previously mentioned crystallography and NMR hydrogen exchange experiments [32, 45]. The crystallography study shows small structural changes in the aromatic cluster II, due to disruption of some of the native interactions in apo-bLA. In order to maintain high values of ionic strength in the experiments above mentioned, NaCl was added to the buffer. Tris, present in the buffer in our experiments, stabilizes LA conformation by simple charge screening effect [46]. Near-UV CD experiments carried out in Tris HCl pH 8.0 with similar charge screening conditions (number of Tris molecules per number of protein molecules) show minor losses of ellipticity of apo-bLA (less than 6% at 270 nm) relatively to native bLA at 5 °C [46]. The observations above indicate that, before UV-illumination, the majority of the apo-bLA molecules in our experiments are in a native-like conformation. The wavelength at maximum Trp fluorescence emission in apo-bLA is the same between 9.3 and 29.9 °C (Fig. 7a and Table 3). It suggests that there should be no considerable differences in the structural stability of apo-bLA molecules in this temperature range.

Continuous 295 nm Trp excitation of apo-bLA leads to an increase in fluorescence emission intensity at 340 nm in the first hours of illumination (Figs. 3 and 6a). Cutinase [17] and horseradish peroxidase [63] display similar fluorescence behavior upon Trp excitation: an increase in fluorescence yield was directly related to light induced damage of strong protein fluorescence quenchers located in close spatial proximity of the proteins' aromatic residues. Fluorescence yield increase in cutinase was caused by light induced cleavage of disulphide bridges mediated by Trp excitation, resulting in a 10-fold increase of fluorescence emission [17]. Free thiol groups are formed upon continuous 295 nm Trp excitation of apo-bLA (Fig. 5), indicating that Trp irradiation induces SS bond breakage. The average

number of thiol groups formed per apo-bLA molecule may be higher than the detected by the Elmann's assay and shown in Fig. 5 (maximum of 0,92 thiol groups formed per apo-bLA molecule) . Previous reports have shown incomplete reaction of protein sulfhydryls with DTNB, due to steric or electrostatic constraints [64–67]. Light induced disruption of SS bonds is correlated with the observed fluorescence emission intensity increase of apo-bLA. Disulphide bridge disruption mediated by UV excitation of aromatic residues in proteins has been previously reported for Ca^{2+} bound goat LA [49, 50]. In calcium bound and apo-goat-LA thiol formation is observed upon continuous Trp excitation but no direct correlation was made between the kinetics of thiol formation and the kinetics of fluorescence emission intensity increase upon UV illumination [49]. Breakage of Cys61-Cys77, Cys73-91 and Cys6-Cys120 has been verified upon continous UV-irradiation of goat LA [49, 50]. All Trp residues contributed to the photolytic cleavage of goat SS bonds. UV-excitation of human LA only yields the disruption of Cys61-Cys77 and Cys73-91 [48]. Breakage of Cys28-Cys111 was not found either in goat or in human LA [48–50].

Trp fluorescence emission is significantly red-shifted upon prolonged 295 nm excitation. The longer the 295 nm excitation time the larger the red-shift: from 7 nm after 1 h to 17 nm after 5 h excitation. This observation is consistent with one or more Trp residues becoming more solvent accessible with illumination time. It suggests a conformational change in apo-LA molecules with Trp excitation, leading to solvent exposure of the protein aromatic clusters. After 5 h of 280 nm (data not shown) and 295 nm illumination, maximum fluorescence emission intensity is observed at ~340 nm (Table 3), a value close to the wavelength of maximum fluorescence emission intensity of partly denaturated bLA at pH 2 (frequently termed classical MG) of ~343 nm [68]. The red shift observed in bLA fluorescence emission when it adopts the mentioned molten globule conformation is due to the movement of the Trp residues into a more solvent-exposed environment compared with native bLA [68]. Far-UV CD spectra of 295 nm illuminated apo-bLA show only minor loss of secondary structural features after 2.8 h of illumination (see Results section). Vanhooren at al. [49] reported similar results for apo-goat-LA in the far-UV region (200–250 nm). It was not feasible to carry out near-UV CD studies in this work, due to the excessive protein concentration required. For such high apo-bLA concentrations, we did not manage to obtain fluorescence emission kinetics similar to the ones here presented. Near-UV CD spectrum of apo-goat-LA showed profound losses of ellipticity (maximally around 270 nm) after excitation of the protein with UV-light [49]. These observations indicate that Trp excitation of apo-bLA and subsequent cleavage of SS bonds induces conformational changes preferentially in the protein's aromatic clusters and that the protein's secondary structure is less affected.

The gradual increase in fluorescence emission intensity here observed can result from conformational changes suffered by apo-bLA upon continuous 295 nm illumination. Quenching groups surround Trp residues in apo-bLA structure including SS bonds, peptide bonds and one histidine residue (see Fig. 1 and Results section). Trp26 is not prone to direct quenching from nearby groups but is subject to indirect quenching by energy transfer to Trp104, through resonance energy transfer. This is supported by experimental observations in goat LA [61]. Trp60 and Trp118 are strongly quenched by nearby SS bonds in goat [61] and human LA [69], which is consistent with the apo-bLA structural features here presented (see Table 1 and Results section). Disulphide bridges are the strongest Trp fluorescence quenching groups [60]. Once broken, SS no longer efficiently quench protein fluorescence. This would explain e.g. an increase in Trp60 fluorescence, upon continuous UV-excitation, assuming that neighbor Cys73-Cys91 and Cys61-Cys77 are also disrupted in apo-bLA. Conformational changes in the aromatic clusters of apo-bLA induced upon UV-excitation may also contribute to an increase in Trp emission intensity due to disruption of the resonance couple Trp26-Trp104, or changes of Trp residues spatial position relatively to the quenching groups.

The observations presented here are correlated with similar fluorescence changes (fluorescence emission increase and red-shift in fluorescence emission spectra) observed upon dithiothreitol chemical reduction of two SS bonds (Cys6-Cys120 and Cys28-Cys111) and all SS bonds in native and apo-bLA [70]. These fluorescence changes have been associated with conformational changes of the protein and formation of MG-like structures [70]. Furthermore, Cys depleted mutant of human LA forms a MG conformation, maintaining most of the native-like structure, more precisely a compact α-domain, showing that the architecture of compact α-helical sub-domain of the protein is determined by the polypeptide sequence and not a direct result of SS bond cross-linking [71]. The correlation between fluorescence emission intensity increase and formation of thiol groups upon 295 nm excitation suggests that the conformational changes on the protein are caused by disulphide bridge disruption, which leads to fluorescence intensity increase. Furthermore, increase in the fluorescence emission intensity and red-shift of the fluorescence emission has also been previously observed when bLA is partly denaturared at pH 2 or when native bLA suffers partial heat denaturation in comparison with native bLA [68]. In these experiments these spectral changes were related to the transition of the protein to MG-like conformations. Fluorescence emission intensity increase as well as a red-shift in fluorescence emission spectra has also

been observed upon UV illumination of Ca^{2+} bound and apo bovine, human and goat LA [48–50], for which light induced cleavage of SS bonds was verified. Trp irradiation of hen egg white lysozyme (a protein structurally homologous to α-lactalbumin [72] induces similar fluorescence changes, which are also related to photolysis of SS bonds of the protein [73].

The progressive loss in normalized excitation intensity upon continuous 295 nm excitation of apo-bLA observed at wavelengths where Trp absorbs (Fig. 4b and c) indicates likely photo-bleaching and/or chemical photo-degradation of Trp specii. The observed red-shift in apo-bLA Trp emission with illumination time also contributes to the observed loss in excitation intensity when emission is set at 320 nm.

As previously mentioned, constant λ_{max} fluorescence emission observed from 9.3 to 29.9 °C indicates that no conformational change has occurred in apo-bLA in this temperature range. The observed 11 nm red-shift in emission of non-illuminated apo-bLA between 29.9 and 34.6 °C (Table 3, Fig. 7a) indicates that a conformational change occurs in apo-bLA before illumination in this temperature interval. Data present in Table 3 and Fig. 7b demonstrates that UV illumination of apo-bLA induced local conformational changes at all temperatures, leading to the same fluorescence emission changes reported at 25 °C: fluorescence emission intensity increase and red-shift in Trp fluorescence emission. The kinetics of fluorescence emission intensity increase at 340 nm upon continuous Trp excitation is faster at higher temperatures (Fig. 7a and Table 2). On the other hand the observed increase in fluorescence emission intensity upon illumination is lower at higher temperatures due to dynamic solvent quenching (Results and Fig. 6a). At 34.6 °C a continuous decrease in fluorescence emission intensity is observed upon 295 nm illumination of apo-bLA, which should be correlated with the conformational transition observed between 29.9 and 34.6 °C in non-illuminated apo-bLA.

The physical interpretation of the exponential equation used for fitting the temperature dependent fluorescence emission time traces is that Trp excited specii are involved in a first order reaction and that the reaction constant is proportional to the rate constant of fluorescence increase (k). For the photo-induced cleavage of SS bonds in cutinase, Neves-Petersen et al. [17] described the fluorescence emission increase using a model that assumes a chemical conversion (1st order photo-induced reaction) of low quantum yield native Trp specii to high quantum yield Trp specii. We consider a similar mechanism for apo-bLA involving the chemical conversion between one pool of molecules with intact disulphide bonds and low fluorescence emission intensity and another with broken SS bonds, MG-like intermediate conformations, and high fluorescence emission intensity. This chemical conversion between the Trp molecules is associated with the increase in Trp fluorescence emission intensity. Thus, the rate of fluorescence emission intensity increase k should be related to the kinetic rate of conversion between the two pools of molecules.

Neves-Petersen et al. have previously reported that the UV-light induced disruption of SS in a protein upon Trp excitation is mediated by the presence of solvated electrons originated from the photoionization of aromatic residues such as Trp and Tyr [10]. Trp photoionization, a major photo-oxidation pathway of many proteins [10, 11] can take place from the pre-fluorescent state S^* and from S_1 giving rise to transient specii (see schemes 1–14) which in proteins will lead to disulphide bridge disruption and free thiol formation. The 21.8 $kJ.mol^{-1}$ Arrhenius activation energy obtained is smaller but comparable to previously reported 50 $kJ.mol^{-1}$ activation energy of thermal photoionization from the singlet excited S_1 of Tryptophan in solution [14]. The presence of other groups (e.g. proton transfer groups, electron acceptors such as disulphide bridges) nearby Trp residues can favor Trp photoionization, lowering the energy barrier required for the reaction, which is correlated with a lower E_a value for Trp photoionization in apo-bLA. Only two decay pathways of excited Trp are known to be favored by a temperature increase: photoionization from S_1 and intramolecular proton transfer from the protonated amino group to the indole ring, not possible in proteins due to the presence of the peptide bond [14]. Photoionization yield has been determined upon measurement of the concentration of generated solvated electron or the concentration of Trp radical formed at each temperature [14]. On the other hand, photoionization yield from higher excited states S^* is known to decrease with temperature [15] and ionization rate constant from S^* is reported to be temperature independent [14]. Furthermore, ^{S*}Trp photoionization in solution yields e_{aq-} within 200 fs after irradiation [12, 13]. ^{S*}Trp photoionization competes with relaxation to S_1. Flash photolysis studies of cutinase and lysozyme show formation of aqueous e_{aq-} within 12 ns after excitation [10]. These observations suggest that Trp photoionization in apo-bLA occurs from S_1. However, delayed detection of solvated electrons after UV excitation of proteins could be due to the fact that Trp is initially buried in the 3D lattice of the protein and not solvent exposed.

Conclusions

Prolonged excitation of Trp residues in apo-bLA induces an increase in fluorescence emission at 340 nm coupled with a red-shift in Trp emission and SS bond disruption. We show that Trp fluorescence spectral changes and disulphide

bridge disruption in apo-bLA are correlated with a chemical conversion between two pools of molecules. Native apo-bLA molecules with intact SS and low fluorescence emission intensity Trp emission are gradually converted into apo-bLA molecules with disrupted disulphide bridges, MG-like conformation, high fluorescence emission intensity and red-shifted Trp emission. A 1st order reaction was an excellent model for the temperature-dependent 340 nm emission kinetic traces. Data suggests that photoionization from the S_1 state is one of the major mechanisms involved in the photolysis of SS in apo-bLA and in the reaction mechanism above described. These studies provide a deeper insight into the photophysical and photochemical processes activated upon UV-illumination proteins.

In the latest years, UV-light (mostly UVC-light – 200–280 nm) has been explored as an alternative method for microbial disinfection of liquid foods, beverages and growth media [74]. Thermal treatment is the traditional method for pasteurization of cheese whey, but has been found to be time consuming and cause denaturation of the whey protein [75, 76]. UV-light continuous sterilization technique of cheese whey and milk has been shown to be effective in eliminating certain microorganisms [75–77]. However, no considerable attention has been given to the potential effects of UV-light on the nutrients present in the UV-pasteurized products. LA constitutes 20–25% of the whey protein [78]. The observations reported in the present paper together with previous reports [48–50] show that UV-light exposure induces structural changes on native and apo-LA. Loss of structure most likely leads to loss in activity, as reported by Vanhooren et al, where ~35% of the original lactose synthase regulatory activity of native goat-LA has been lost after 3 h of 290 nm illumination [50]. Furthermore, Elmnaser et al. recently reported some structural changes upon light treatment (including UV-light) of milk proteins [79]. A more careful analysis should be undertaken when studying UV-light as an alternative for pasteurization and sterilization processes in whey and other milk derivatives where LA is present since the biological function of the protein might also be affected, and protein denaturation may occur as well. Experimental parameters such as UV-irradiation power and illumination time of the medium should be optimized in order to ensure microorganism destruction but avoiding affecting the structure and the function of whey protein. This same concern should be extended to all protein containing food products.

Acknowledgments M.C. acknowledges the support from "Fundação para a Ciência e Tecnologia" (FCT) for the PhD grant (SFRH/BD/61012/2009) supported by "Programa Operacional Potencial Humano" (POPH) in the framework of "Quadro de Referência Estratégico Nacional" (QREN) and co-financed by the European Social Fund ("Fundo Social Europeu", FSE).

References

1. Bent DV, Hayon E (1975) Excited-state chemistry of aromatic amino-acids and related peptides .3. tryptophan. J Am Chem Soc 97(10):2612–2619
2. Creed D (1984) The photophysics and photochemistry of the near-UV absorbing amino-acids .1. Tryptophan and its simple derivatives. Photochem Photobiol 39(4):537–562
3. Bent DV, Hayon E (1975) Excited-state chemistry of aromatic amino-acids and related peptides .1.tyrosine. J Am Chem Soc 97 (10):2599–2606
4. Creed D (1984) The photophysics and photochemistry of the near-uv absorbing amino-acids .2. Tyrosine and its simple derivatives. Photochem Photobiol 39(4):563–575
5. Bent DV, Hayon E (1975) Excited-state chemistry of aromatic amino-acids and related peptides .2.phenylalanine. J Am Chem Soc 97(10):2606–2612
6. Creed D (1984) The photophysics and photochemistry of the near-UV absorbing amino-acids.3. Cystine and its simple derivatives. Photochem Photobiol 39(4):577–583
7. Du H, Fuh RA, Li J, Corkan A, Lindsey JS (1998) PhotochemCAD: a computer-aided design and research tool in photochemistry. Photochem Photobiol 68(2):141–142
8. Robbins RJ, Fleming GR, Beddard GS, Robinson GW, Thistlethwaite PJ, Woolfe GJ (1980) Photophysics of aqueous tryptophan: pH and temperature effects. J Am Chem Soc 102(20):6271–6279
9. Tsentalovich YP, Snytnikova OA, Sagdeev RZ (2004) Properties of excited states of aqueous tryptophan. J Photochem Photobiol A: Chem 162(2–3):371–379
10. Neves-Petersen MT, Klitgaard S, Pascher T, Skovsen E, Polivka T, Yartsev A, Sundström V, Petersen SB (2009) Flash photolysis of cutinase: identification and decay kinetics of transient intermediates formed upon UV excitation of aromatic residues. Biophys J 97(1):211–226
11. Devies MJ, Truscott RJW (2001) Photo-oxidation of proteins and its role in cataractogenesis. J Photochem Photobiol B: Biol 63(1–3):114–125
12. Mialocq JC, Amouyal E, Bernas A, Grand D (1982) Picosecond laser photolysis of aqueous indole and tryptophan. J Phys Chem 86(16):3173–3177
13. Peon J, Hess GC, Pecourt J-ML, Yuzawa T, Kohler B (1999) Ultrafast photoionization dynamics of indole in water. J Phys Chem 103(14):2460–2466
14. Sherin PS, Snytnikova OA, Tsentalovich YP (2004) Tryptophan photoionization from prefluorescent and fluorescent states. Chem Phys Lett 391(1–3):44–49
15. Sherin PS, Snytnikova OA, Tsentalovich YP (2006) Competition between ultrafast relaxation and photoionization in excited prefluorescent states of tryptophan and indole. J Chem Phys 125 (14):144511
16. Kerwin BA, Remmele RL Jr (2006) Protect from light: photodegradation and protein biologics. J Pharmac Sci 96(6):1468–1479
17. Neves-Petersen MT, Gryczynski Z, Lakowicz J, Fojan P, Pedersen S, Petersen E, Petersen SB (2002) High probability of disrupting a disulphide bridge mediated by an endogenous excited tryptophan residue. Protein Sci 11(3):588–600
18. Hoffman MZ, Hayon E (1972) One-electron reduction of the disulfide linkage in aqueous solution. Formation, protonation, and decay kinetics of the RSSR- radical. J Am Chem Soc 94(23):7950–7957

19. Neves-Petersen MT, Snabe T, Klitgaard S, Duroux M, Petersen SB (2006) Photonic activation of disulfide bridges achieves oriented protein immobilization on biosensor surfaces. Protein Sci 15(2):343–351
20. Skovsen E, Kold AB, Neves-Petersen MT, Petersen SB (2009) Photonic immobilization of high-density protein arrays using Fourier optics. Proteomics 9(15):3945–3958
21. Parracino A, Gajula GP, Gennaro AK, Correia M, Neves-Petersen MT, Rafaelsen J, Petersen SB (2010), Photonic immobilization of BSA for nanobiomedical applications: creation of high density microarrays and superparamagnetic bioconjugates. Biotechnol Bioeng. 2010 Dec 1. [Epub ahead of print]
22. Parracino A, Neves-Petersen MT, di Gennaro AK, Pettersson K, Lövgren T, Petersen SB (2010) Arraying prostate specific antigen PSA and Fab anti-PSA using light-assisted molecular immobilization technology. Protein Sci 19(9):1751–1759
23. Duroux M, Skovsen E, Neves-Petersen MT, Duroux L, Gurevich L, Petersen SB (2007) Light-induced immobilisation of biomolecules as a replacement for present nano/micro droplet dispensing based arraying technologies. Proteomics 7(19):3491–3499
24. Snabe T, Røder GA, Neves-Petersen MT, Petersen SB, Buus S (2006) Oriented coupling of major histocompatibility complex (MHC) to sensor surfaces using light assisted immobilisation technology. Biosens Bioelectron 21(8):1553–1559
25. Neves-Petersen MT, Snabe T, Klitgaard S, Duroux M, Petersen SB (2006) Photonic Biosensors: UV light induced molecular switch allows sterically oriented immobilisation of biomolecules and the creation of protein nanoarrays. Protein Sci 15(2):343–351
26. Duroux M, Duroux L, Neves-Petersen MT, Skovsen E, Petersen SB (2007) Novel photonic technique creates micrometer resolution protein arrays and provides a new approach to coupling of genes, peptide hormones and drugs to nanoparticle carriers. Appl Surf Sci 253(19):8125–8129
27. Duroux M, Gurevich L, Neves-Petersen MT, Skovsen E, Duroux L, Petersen SB (2007) Using light to bioactivate surfaces: a new way of creating oriented, active immunobiosensors. Appl Surf Sci 254(4):1126–1130
28. Skovsen E, Duroux M, Neves-Petersen MT, Duroux L, Petersen SB (2007) Molecular printing using UV-assisted immobilization of biomolecules. Int J Optomechatronics 1(4):383–391
29. Neves-Petersen MT, Duroux M, Skovsen E, Duroux L, Petersen SB (2009) Printing novel architectures of nanosized molecules with micrometer resolution using light. J Nanosci Nanotechnol 9 (6):3372–3381
30. Skovsen E, Neves-Petersen MT, Kold A, Duroux L, Petersen SB (2009) Immobilizing biomolecules near the diffraction limit. J Nanosci Nanotechnol 9(7):4333–4337
31. Skovsen E, Kold A, Neves-Petersen MT, Petersen SB (2009) Photonic immobilization of high density protein arrays using fourier optics. Proteomics 9(15):1–4
32. Chrysina ED, Brew K, Acharya KR (2000) Crystal structures of apo- and holo-bovine alpha-lactalbumin at 2.2-Å resolution reveal an effect of calcium on inter-lobe interactions. J Biol Chem 275 (47):37021–37029
33. Permyakov EA, Berliner LJ (2000) α-Lactalbumin: structure and function. FEBS Lett 473(3):269–274
34. Ramakrishnan B, Qasba PK (2001) Crystal structure of lactose synthase reveals a large conformational change in its catalytic component, the b1,4-Galactosyltransferase-I. J Mol Biol 310 (1):205–218
35. Kuwajima K (1996) The molten globule state of α-lactalbumin. FASEB J 10(1):102–109
36. Laureto PP, Frare E, Gottardo R, Fontana A (2002) Molten globule of bovine α-Lactalbumin at neutral pH induced by heat, trifluoroethanol, and oleic acid: a comparative analysis by circular dichroism spectroscopy and limited proteolysis. PROTEINS: Structure, Function, and Genetics 49(3):385–397
37. Cawthern KM, Permyakov E, Berliner LJ (1996) Membrane-bound states of alpha-lactalbumin: implications for the protein stability and conformation. Protein Sci 5(7):1394–1405
38. Aits S, Gustafsson L, Hallgren O, Brest P, Gustafsson M, Trulsson M, Mossberg AK, Simon HU, Mograbi B, Svanborg C (2009) HAMLET (human alpha-lactalbumin made lethal to tumor cells) triggers autophagic tumor cell death. Int J Cancer 124(5):1008–1019
39. Rammer P, Groth-Pedersen L, Kirkegaard T, Daugaard M, Rytter A, Szyniarowski P, Høyer-Hansen M, Klitgaard Povlsen L, Nylandsted J, Larsen JE, Jäättelä M (2010) BAMLET Activates a lysosomal cell death program in cancer cells. Mol Cancer Ther 9 (1):24–32
40. Pettersson-Kastberg J, Mossberg AK, Trulsson M, Yong YJ, Min S, Lim Y, O'Brien JE, Svanborg C, Mok KH (2009) alpha-Lactalbumin, engineered to be nonnative and inactive, kills tumor cells when in complex with oleic acid: a new biological function resulting from partial unfolding. J Mol Biol 394(5):994–1010
41. Hendrix TM, Griko YV, Privalov PL (1996) Energetics of structural domains in α-lactalbumin. Protein Sci 5(5):923–931
42. Pfeil W (1998) Is the molten globule a third thermodynamic state of proteins? The example of alpha-lactalbumin. Prot Struct Funct Genet 30(1):43–48
43. Veprintsev DB, Permyakov SE, Permyakov EA, Rogov VV, Cawtherm KM, Berliner LJ (1997) Cooperative thermal transitions of bovine and human apo-lactalbumins: evidence for a new intermediate state. FEBS Lett 412(3):625–628
44. Wilson G, Ford SJ, Cooper A, Hecht L, Wen ZQ, Barron LD (1995) Vibrational Raman optical activity of a-lactalbumin: comparison with lysozyme, and evidence for native tertiary folds in molten globule states. J Mol Biol 254(4):747–760
45. Wijesinha-Bettoni R, Dobson CM, Redfield C (2001) Comparison of the structural and dynamical properties of holo and apo bovine alpha-lactalbumin by NMR spectroscopy. J Mol Biol 307(3):885–898
46. Griko YV, Remeta DP (1999) Energetics of solvent and ligand-induced conformational changes in alpha-lactalbumin. Protein Sci 8(3):554–561
47. Jr O, Halskau R, Perez-Jimenez B, Ibarra-Molero J, Underhaug V, Muñoz AM, Sanchez-Ruiz JM (2008) Large-scale modulation of thermodynamic protein folding barriers linked to electrostatics. Proc Natl Acad Sci U S A 105(25):8625–8630
48. Permyakov EA, Permyakov SE, Deikus GY, Morozova-Roche LA, Grishchenko VM, Kalinichenko LP, Uversky VN (2003) Ultraviolet Illumination-induced Reduction of α-Lactalbumin disulfide bridges. PROTEINS: Structure, Function, and Genetics 51(4):498–503
49. Vanhooren A, Devreese B, Vanhee K, Van Beeumen J, Hanssens I (2002) Photoexcitation of tryptophan groups induces reduction of two disulfide bonds in goat α-Lactalbumin. Biochemistry 41 (36):11035–11043
50. Vanhooren A, De Vriendt K, Devreese B, Chedad A, Sterling A, Van Dael H, Van Beeumen J, Hanssens I (2006) Selectivity of tryptophan residues in mediating photolysis of disulfide bridges in goat α-Lactalbumin. Biochemistry 45(7):2085–2093
51. Masaki K, Masuda R, Takase K, Kawano K, Nitta K (2000) Stability of the molten globule state of a domain-exchanged chimeric protein between human and bovine α-lactalbumins. Protein Engineering 13(1):1–4
52. Riener CK, Kada G, Gruber HJ (2002) Quick measurement of protein sulfhydryls with Ellman's reagent and with 4,4′-dithiodipyridine. Anal Bioanal Chem 373:266–276
53. Riddles PW, Blakeley RL, Zerner B (1983) Reassessment of Ellman's reagent. Meth Enzymol 91:49–60
54. Tsodikov OV, Record MT Jr, Sergeev YV (2002) A novel computer program for fast exact calculation of accessible and molecular surface areas and average surface curvature. J Comput Chem 23(6):600–609

55. Richards FM (1977) Areas, volumes, packing and protein structure. Annu Rev Biophys Bioeng 6:151–176
56. Miller S, Janin J, Lesk AM, Chothia C (1987) Interior and surface of monomeric proteins. J Mol Biol 196(3):641–656
57. Mok KH, Nagashima T, Day IJ, Hore PJ, Dobson CM (2005) Multiple subsets of side-chain packing in partially folded states of alpha-lactalbumins. Proc Natl Acad Sci U S A 102(25):8899–8904
58. Li A-J, Nussinov R (1998) A set of van der waals and coulombic radii of protein atoms for molecular and solvent-accessible surface calculation, packing evaluation, and docking. PROTEINS: Structure, Function, and Genetics 32(1):111–127
59. Loewenthal R, Sancho J, Fersht AR (1991) Fluorescence spectrum of barnase: contributions of three tryptophan residues and a histidine-related pH dependence. Biochemistry 30 (27):6775–6779
60. Van Gilst M, Hudson BS (1996) Histidine-tryptophan interactions in T4 lysozyme: 'Anomalous' pH dependence of fluorescence. Biophys Chem 63(1):17–25
61. Vanhooren A, Illyes E, Majer Z, Hanssens I (2006) Fluorescence contributions of the individual Trp residues in goat alpha-lactalbumin. Biochim Biophys Acta 1764(10):1586–1591
62. Engel MFM, van Mierlo CPM, Visser AJWG (2002) Kinetic and Structural Characterization of Adsorption-induced Unfolding of Bovine α-Lactalbumin. J Biol Chem 277(13):10922–10930
63. Neves-Petersen MT, Klitgaard S, Carvalho ASL, Petersen SB, de Barros MRA, Pinho e Melo E (2007) Photophysics and Photochemistry of Horseradish Peroxidase A2 upon Ultraviolet Illumination. Biophys J 92(6):2016–2027
64. Grassetti DR, Murray JF Jr (1967) Determination of sulfhydryl groups with 2,2'- or 4,4'-dithiodipyridine. Arch Biochem Biophys 119(1):41–49
65. Han MK, Roseman S, Brand L (1990) Sugar transport by the bacterial phosphotransferase system. Characterization of the sulfhydryl groups and site-specific labeling of enzyme I. J Biol Chem 265(4):1985–1895
66. Wilson JM, Wu D, Motiu-DeGrood R, Hupe DJ (1980) A spectrophotometric method for studying the rates of reaction of disulfides with protein thiol groups applied to bovine serum albumin. J Amer Chemic Soc 102(1):359–363
67. Woodward J, Tate J, Herrmann PC, Evans BR (1993) Comparison of Ellman's reagent with N-(1-pyrenyl)maleimide for the determination of free sulfhydryl groups in reduced cellobiohydrolase I from Trichoderma reesei. J Biochem Biophys Methods 26(2–3):121–129
68. Wijesinha-Bettoni R, Gao C, Jenkins JA, Mackie AR, Wilde PJ, Mills EN, Smith LJ (2007) Heat treatment of bovine alpha-lactalbumin results in partially folded, disulfide bond shuffled states with enhanced surface activity. Biochemistry 46(34):9774–9784
69. Chakraborty S, Ittah V, Bai P, Luo L, Haas E, Peng ZY (2001) Structure and dynamics of the alpha lactalbumin molten globule: fluorescence studies using proteins containing a single tryptophan residue. Biochemistry 40(24):7228–7238
70. Ewbank JJ, Creighton TE (1993) Structural characterization of the disulfide folding intermediates of bovine alpha-lactalbumin. Biochemistry 32(14):3694–3707
71. Redfield C, Schulman BA, Milhollen MA, Kim PS, Dobson CM (1999) Alpha-lactalbumin forms a compact molten globule in the absence of disulfide bonds. Nat Struct Biol 6(10):948–952
72. Qasba PK, Kumar S (1997) Molecular divergence of lysozymes and alpha-lactalbumin. Crit Rev Biochem Mol Biol 32(4):255–306
73. Wu L-Z, Sheng Y-B, Xie J-B, Wang W (2008) Photoexcitation of tryptophan groups induced reduction of disulfide bonds in hen egg white lysozyme. J Molec Struct 882(1–3):101–106
74. Koutchma T (2009) Advances in ultraviolet light technology for non-thermal processing of liquid foods. Food Bioprocess Technol 2(2):138–155
75. Mahmoud NS, Ghaly AE (2004) On-line sterilization of cheese whey using ultraviolet radiation. Biotechnol Prog 20(2):550–560
76. Singh JP, Ghaly AE (2006) Reduced fouling and enhanced microbial inactivation during online sterilization of cheese whey using UV coil reactors in series. Bioprocess Biosyst Eng 29 (4):269–281
77. Altic LC, Rowe MT, Grant IR (2007) UV light inactivation of Mycobacterium avium subsp. paratuberculosis in milk as assessed by FASTPlaqueTB phage assay and culture. Appl Environ Microbiol 73(11):3728–3733
78. Hong Y-H, Creamer LK (2002) Changed protein structures of bovine β-lactoglobulin B and α-lactalbumin as a consequence of heat treatment. Int Dairy J 12:345–359
79. Elmnasser N, Dalgalarrondo M, Orange N, Bakhrouf A, Haertlé T, Federighi M, Chobert JM (2008) Effect of pulsed-light treatment on milk proteins and lipids. J Agric Food Chem 56(4):1984–1991